Are stress distributions along faults the signature of asperity squeeze?

J. Schmittbuhl, Guillaume Chambon, A. Hansen, Michel Bouchon

Are stress distributions along faults the signature of asperity squeeze?

J. Schmittbuhl,[1] G. Chambon,[2] A. Hansen,[3] and M. Bouchon[4]

Received 22 February 2006; revised 1 May 2006; accepted 17 May 2006; published 7 July 2006.

[1] We propose a possible model for the origin of the spatial fluctuations of the stress field along faults and test our model in the case of the Nojima fault, Japan where unique estimates of the absolute stress field have been obtained. The model consists of two parts: an up-scaling of the fault morphology measured at laboratory scales and a numerical computation using a boundary element approach of the influence on the stress field along the fault of an elastic squeeze of the fault asperities. Accordingly, fluctuations of the stress field along the fault would be dominated by quenched fault properties rather than dynamical stress fluctuations produced during earthquakes. **Citation:** Schmittbuhl, J., G. Chambon, A. Hansen, and M. Bouchon (2006), Are stress distributions along faults the signature of asperity squeeze?, *Geophys. Res. Lett.*, *33*, L13307, doi:10.1029/2006GL025952.

1. Introduction

[2] Numerous recent studies have been proposed to reconstruct slip and stress histories along faults during large earthquakes [e.g., *Tinti et al.*, 2005]. Even if different inversions for the same fault show discrepancies, co-seismic slip and stress drop distributions usually exhibit very heterogeneous patterns [*Mai and Beroza*, 2002; *Lavallée and Archuleta*, 2005]. Such observations suggest that either dynamical processes during earthquakes roughen the stress fields, or that strong heterogeneities of the stress field persist along the fault over the seismic cycle. Each hypothesis leads to very different modelling of seismic hazard. Indeed the first case requires a careful description of the mechanical instability and of the earthquake dynamics. In the second case, on the contrary, a precise analysis of the fault structure is required. To choose among these assumptions, estimates of the absolute stress field along the fault are required though they are rather difficult to obtain.

[3] The 1995 Kobe, Japan, earthquake is a unique case where the absolute stress field has been recovered with a sufficiently high spatial resolution [*Bouchon et al.*, 1998]. The estimate of the absolute stress field in Figure 1 relies on the rotation of the slip vector during the earthquake and the requirements of co-linearity between the directions of maximum shear stress and instantaneous slip [*Spudich*, 1992]. The grid size of estimated values is 61×22 with a spatial resolution of 1 km $\times$ 1 km. Stress estimates are obtained from the inverted slip distribution along the fault [*Bouchon et al.*, 1998] assuming that the friction is isotropic and that the instantaneous slip direction is the direction of maximum shear stress. The slip inversion computation implies an interpolation but only limited to the lowest scales (<5km).

[4] The absolute initial stress field shows significant spatial fluctuations (see Figure 1). The average initial stress estimated over the inversion region is rather low: 3.3 MPa with rms fluctuations of the same order: 1.9 MPa. Average final stress are: 1.6 ± 1.2 MPa. Main asperities are is of the order of 10 km and with an isotropic distribution. It is of interest to note that although magnitudes of the peaks are smaller in the final case, their positions are persistent with respect to the initial stress field (except at large depth around 20 km where local maxima of the initial stress are significantly reduced by the earthquake - this area is however the region of weakest resolution). Accordingly, a significant part of the heterogeneities of the stress field is quenched along the fault, and only weakly modified by dynamical stress fluctuations that result from earthquake propagation.

[5] Micro-earthquake activity is another possible signature of structural asperities along the fault [*Rubin et al.*, 1999]. The case of the Izmit region, Turkey around the 1999 Kocaeli, earthquake is a good example. Indeed, a significant activity has been monitored before the main event [*Bariş et al.*, 2002] and followed after the earthquake [*Özalaybey et al.*, 2002].

[6] In this letter, we propose a possible mechanism for the origin of the stress fluctuations along the fault. We attempt to link the stress field distribution to the roughness of the fault plane. This is based on the analysis of the transformation of fault asperities when submitted to a normal load. We limit ourselves to an elastic deformation of the topography which might be dominant at large scales. In doing so, we ignore plastic strain which might occur locally on small asperities. We however include the broad range of asperity size as observed on natural fault surfaces.

2. Fault Roughness

[7] Roughness of the fault plane has been largely studied both at laboratory scale [*Scholz*, 1997; *Power and Durham*, 1997] and at field scale [*Power et al.*, 1987; *Schmittbuhl et al.*, 1993]. We complete here former results at laboratory scales with the measurement of the topography of two fault planes: one extracted from the Bastille Hill fault (BF) near the city of Grenoble, France and the second one from the Aegion fault (AF) in the Gulf of Corinth, Greece. An optical profiler has been used with a resolution of 3 μm for positions along the mean fracture plane and of 1 μm for height estimates [*Renard et al.*, 2004]. The grid was 4100×873 for BF and 2050×2050 for AF, with a mesh of 24 μm $\times$ 24 μm.

[8] Analysis of the roughness has been performed using the rms topography at scale l: $\sigma(l)$ [*Schmittbuhl et al.*,

[1]Institut de Physique du Globe de Strasbourg, Strasbourg, France.
[2]Cemagref, Grenoble, France.
[3]Norges Teknisk-Naturvitenskapelige Universitet, Trondheim, Norway.
[4]Laboratoire de Géophysique Interne et Tectonique, Grenoble, France.

0094-8276/06/2006GL025952

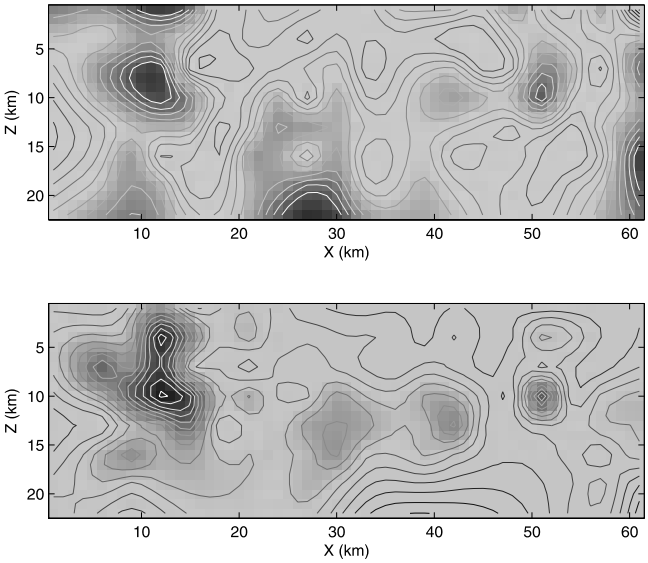

Figure 1. Absolute shear stress distributions along the Nojima Fault, Japan: (top) before (initial stress) and (bottom) after (final stress) the Kobe, 1995 Earthquake (modified after *Bouchon et al.* [1998]). Dark gray areas correspond to local maxima, x- and z- axes are respectively horizontal and vertical directions. These distributions show persistent spatial fluctuations: relative maxima are located at similar positions along the fault plane (except at large depth).

1995a, 1995b]. A power law behavior with a slope that defines the Hurst exponent of the fault roughness, is very consistent with the data over three decades (see Figure 2). We obtained $H_r = 0.81 \pm 0.03$ for BF and $H_r = 0.76 \pm 0.03$ for AF. These results are similar to other measurements [e.g., *Scholz*, 1997]. Moreover, the results obtained at laboratory scales is also valid at field scale [*Schmittbuhl et al.*, 1993; *Renard et al.*, 2006] thus providing a geometrical model of fault topography at all scales.

[9] To get a full description of the fault asperity geometry, the prefactor of the scaling function has also to be characterized. For instance, using the standard deviation of the height differences over a length scale Δx, the prefactor can be defined as: $\sigma(\Delta x) = l_r^{1-H}\Delta x^H$ where H is the Hurst exponent and the prefactor l_r is the topothesy of the fault roughness [*Simonsen et al.*, 2000]. The latter is a characteristic length scale along x for which typical fluctuations of the roughness are of the same order: $\sigma(l_r) = l_r$. In other words, l_r is the typical length scale to get a 45° slope. The topothesy of the measured fault planes is very small: $l_r \approx 3\ 10^{-6}$m for BF and $l_r \approx 3\ 10^{-7}$m for AF, meaning that fault surfaces are rather smooth.

[10] We confirmed our results by using an independent technique: the Average Wavelet Coefficient technique [*Simonsen et al.*, 1998]. It starts from the wavelet transform along horizontal stress profiles:

$$W_{a,b} = \frac{1}{\sqrt{a}} \int_{-\infty}^{+\infty} dx\ \psi\left(\frac{x-b}{a}\right) |\tau(x, z = const)| \qquad (1)$$

where ψ is in our case a Daubechies-4 wavelet. Wavelet coefficients are then averaged over the translation factor b for each length scale a: $W_a = \langle W_{a,b} \rangle_b$. For a self-affine field, the average wavelet coefficient scales as: $W_a \propto a^{H_\tau+1/2}$. The topothesy could similarly be defined from the wavelet spectrum: $W(a) = a_r^{1-H}\ a^{1/2+H}$ with $W^{2/3}(a_r) = a_r$. We obtained for the fault roughness, $a_r = 9\ 10^{-5}$m for BF and $a_r = 2\ 10^{-10}$m for AF.

[11] Despite the relatively large scattering of the fault topothesy values, it is possible to get an estimate of the magnitude of fault asperities at field scale, from the scaling property of the measured fault roughness at laboratory scale. For instance, at a kilometric scale, $\sigma(1\text{ km}) \approx 5-20$m and at a 60 km scale, like the inverted region extension for Kobe earthquake (Figure 1), $\sigma(60\text{km}) \approx 100-600$m. This shows that the fault is essentially flat at large scale (i.e., small aspect ratio $\sigma_u(\Delta x)/\Delta x = l_r^{0.2}\ \Delta x^{-0.2}$) but still includes a large scale pattern of small magnitude asperities.

3. Asperity Squeeze Model

[12] The first step in the link between topography and stress, is to estimate the normal stress field from the full squeeze of the fault asperities. The difficult part consists in the non independence of the asperities during deformation owing to their strong spatial correlations and the long range elastic coupling. The approach is based on the work of *Hansen et al.* [2000] and *Batrouni et al.* [2002] which consists of a boundary element modeling of the elastic deformation of a rough interface using Fourier acceleration. The code provides an estimate of the normal stress distribution when squeezing a rigid rough surface against a elastic half space which is an equivalent problem to two rough elastic surfaces in contact. Therefore, it transforms geometrical asperities under a free boundary condition to an elastically loaded interface in partial or full contact with or without cohesion. It converges iteratively toward a mechanical equilibrium of the interface which is submitted to mixed boundary conditions: imposed displacement for the contacts

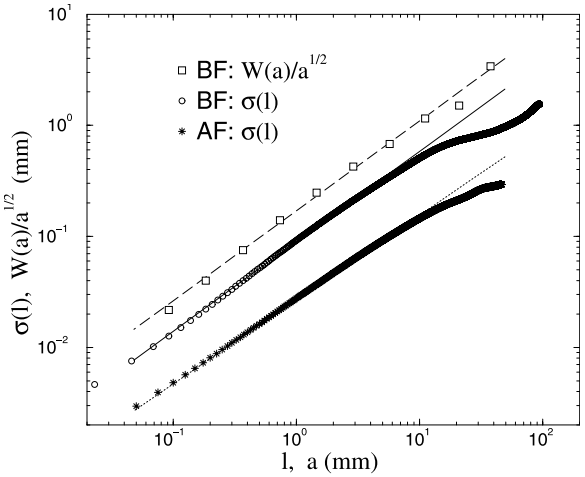

Figure 2. Scaling of fault roughness at laboratory scale. Two fault plane are sampled: the Bastille hill fault, Grenoble, France (BF) and the Aegion fault, Greece (AF). Fits are: $W(a)/a^{1/2} = 0.17\ a^{0.81}$ and $\sigma(l) = 0.09\ l^{0.81}$ for the Bastille Fault and $\sigma(l) = 0.027\ l^{0.76}$ for the Aegion fault.

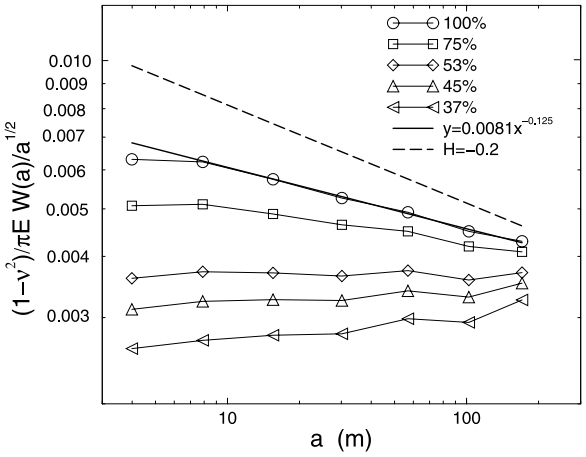

Figure 3. Scaling of dimensionless normal stress field when squeezing the fault roughness elastically (E is the Young modulus and ν is the Poisson coefficient). Normalized AWC spectrum are computed for different imposed normal displacements applied to the fault. The grid is 512 × 512. Magnitude of the normal load is monitored from the ratio of the effective area of contact to the total area of the interface (i.e., full contact is 100%). The roughness of the deformed topography has the same scaling as for Aegion Fault (AF).

and imposed stress for non contact areas. Figure 3 presents the AWC spectrum of the produced stress field for different normal load in the case of a synthetic fault with properties equal to that measured at laboratory scale ($l_r = 3\ 10^{-7}$ and $H_r = 0.8$) without cohesion along the fault. At full contact and with cohesion, the Hurst exponent of the normal stress field H_σ approaches: $H_\sigma = H_r - 1$ as shown by *Hansen et al.* [2000]. It is of interest to note that under the conditions of full contact, the scaling exponent becomes negative. Accordingly, the fluctuations of the stress field increases when scale decreases. For instance, in the case of a scaling valid over a very large range of length scales, e.g., from a submillimeter scale to 100 km scale, the ratio of the stress fluctuations estimated at these two different scales, could be as small as: $\sigma_\sigma(100\text{km})/\sigma_\sigma(0.1\text{mm}) \approx 10^{-2}$. If partial contact takes place, the effective Hurst exponent is evolving with load from positive at smaller load to negative at higher load.

[13] As a second step, we propose that the fault asperity squeeze process could be a possible mechanism for explaining the general feature of the stress field along faults at the onset of an earthquake. Indeed, we assume that a friction law exists along the fault that locally relates the shear stress τ to the normal stress σ: $\tau = \mu\sigma$ with a friction coefficient μ. On this basis, the average shear stress field is related to the distribution of the friction coefficient and that of the normal stress: $\langle\tau\rangle_{fault} = \langle\mu \cdot \sigma\rangle_{fault}$. The simplest assumption is to consider that the friction coefficient is constant like for a Coulomb criterion. In this case, the shear stress is simply proportional to the normal stress, and the self-affine scaling of the normal stress field also applies to the shear stress: $H_\tau = H_\sigma$. Hence we predict that the Hurst exponent of the shear stress is $H_\tau = H_r - 1 \approx -0.2$ if the Hurst exponent of the fault roughness is $H_r \approx 0.8$.

[14] The knowledge of the scaling of the stress field allows us to produce synthetic stress fields that reproduce observed fluctuations. Figure 4 shows an example of two synthetic stress fields computed using a similar grid to observed data and a similar stress magnitude (same average stress and same rms). The upper plot is a smoothed stress field with a smoothing at small scales similar to inverted data. The stress field is computed from the fractional integration of a white noise in the Fourier domain. Indeed a self-affine surface with an Hurst exponent H has 1D power spectra with a slope $s = -1 - 2H$ in a log-log plot. Accordingly, after producing a white noise with a flat power spectrum, its 2D Fourier transform is multiplied by the factor: k^{-1-H} where k is the wavenumber [*Méheust and Schmittbuhl*, 2001; *Lavallée and Archuleta*, 2003]. An inverse Fourier transform provides the synthetic stress field as shown in Figure 4. The second plot in Figure 4 is without smoothing and represents an extended scaling down to the grid size (the kilometer scale). Fluctuations are significantly larger at small scales and display anti-persistent correlations. Such a behavior is expected to be generic for squeeze-induced normal and shear stresses, since roughness exponents of fault surfaces are systematically below unity for a wide range of scales.

4. Case of the Nojima Fault, Japan

[15] In terms of stress magnitude, our stress computation predicts (using the prefactor of the fit of Figure 3 for AF with $l = 10^5$) that the magnitude of the stress field at large scale (i.e., 100km) and with a full asperity squeeze and a cohesion condition (i.e., $H_\tau = -0.2$), would be of the order of: $\sigma_\tau(100\text{ km}) = 8\ 10^{-4}\ \pi\mu E/(1-\nu^2)$. Classical values of E, ν and μ: $E = 3\ 10^{10}\ Pa$, $\nu = 0.25$ and $\mu = 0.6$, lead to $\sigma_\tau(100\text{ km}) \approx 50$ MPa instead of the 2MPa measured along the Nojima fault. Let us first recall that the average stress along the Nojima fault is very low compared to classical estimates. Second the prefactor in σ_τ estimate is proportional to the roughness topothesy l_r. A lower magnitude of the topothesy of the Nojima fault could contribute to a lower prediction of σ_τ. Otherwise, a lower E modulus at large scale or a more complex friction coefficient distribution could also explain some of the difference. Moreover we did not account for any yield stress though plastic strain definitively develops at local scale during asperity squeeze under large load. These aspects will be included in a forthcoming work.

[16] To describe the scaling of the heterogeneities of the stress field $\tau(x, z)$, presented in Figure 1, where x and z are respectively the horizontal and vertical coordinates, we search for possible spatial correlations of the stress fluctuations. Along horizontal profiles, we computed the auto-correlation function of the local stress estimates. More precisely, we looked for power law auto-correlation functions. Indeed, if the auto-correlation function of a stress profile is a power law and scales as: $\langle\tau(x), \tau(x+d)\rangle_x \propto d^{2H_\tau}$, then the stress field is self-affine with H_τ the Hurst exponent if multi-affinity is excluded.

[17] One way to estimate the auto-correlation function is to compute the power spectrum which is its Fourier transform. Figure 5 shows the power spectra of the of initial and final stress profiles along x in a log-log plot. Though the

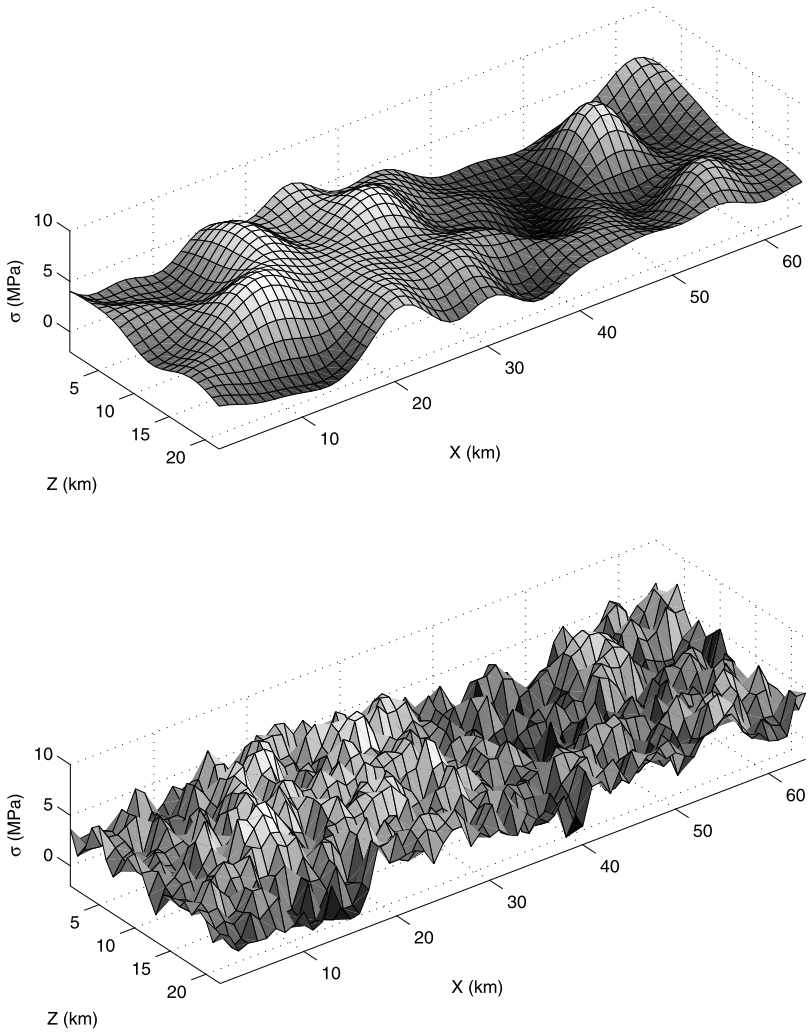

Figure 4. Example of a synthetic stress field produced from a self-affine distribution with a Hurst exponent $H_\tau = -0.2$. (top) A similar interpolation to observed data at small scales is introduced. (bottom) No smoothing at small scales is done.

absolute stress fields obtained for the Kobe earthquake present the best resolution accessible with existing seismological data, only limited ranges of scaling are available. Two regimes can be proposed: at small scales, i.e., large wave numbers, (between 1km and 5km) the behavior can be attributed to data interpolation and resolution limitations. At large scales, i.e., low wave numbers, (above 5 km), a power law with an exponent 0.7 ± 0.1 is a possible fit. The latter indicates a self-affine behavior with a negative Hurst exponent of $H_\tau = -0.15 \pm 0.1$. An uncorrelated noise would show a Hurst exponent $H = -0.5$, i.e., a flat horizontal behavior in Figure 5 [*Hansen et al.*, 2001]. Accordingly, stress fluctuations are weakly correlated but sufficiently to be non independent. Moreover a negative Hurst exponent means that fluctuations are larger at small scales than at large scales. It is important to note that the proposed fit at large scales is valid for both the initial and final stress fields. This is consistent with the persistence of the stress field because of quenched structures along the fault.

[18] The prediction of the squeeze model compares well with what has been obtained at large scale (i.e., above the smoothing length scale) for the Kobe earthquake as shown

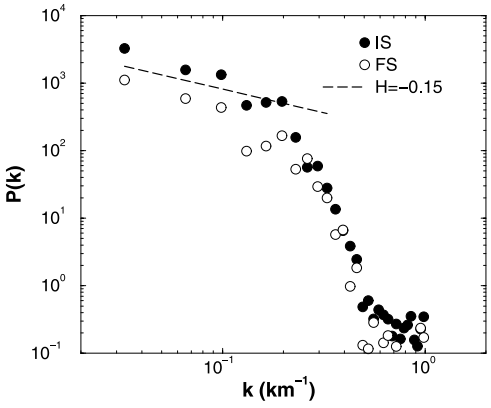

Figure 5. Power spectra of the horizontal stress profiles averaged over the 10 first kilometers: IS for initial stress field and FS for final stress field (shown in Figure 1).

in Figure 5. It also implies, as mentioned earlier, that the magnitude of the shear stress fluctuations could be larger locally than at large scale. Indeed, rms of the stress field filtered at scale l, evolves as: $\sigma_\tau(l) \propto l^{-0.2}$.

5. Conclusions

[19] In conclusion, we analyzed the 1995 Kobe earthquake for which it has been possible to reconstruct not only the relative stress field during the event (stress drop), but also the absolute stress field [*Bouchon et al.*, 1998]. It appears that distributions of initial and final stresses before and after the earthquake, show strong similarities. This suggests that the stress distribution constitutes an intrinsic property of Nojima fault, and is only slightly affected by earthquakes. Shear stresses along Nojima fault exhibit strong spatial variability.

[20] Despite a small range of resolution, the power spectrum of the stress field is shown to be consistent with a self-affine scaling with a slightly negative Hurst exponent ($H_\tau = -0.2$) that comes from the elastic squeeze of upscaled fault asperities.

[21] **Acknowledgments.** We acknowledge ACIs RNCC and ALEAS, and ANR MODALSIS of the French Ministry of Research, in addition to the Norwegian Research Council for support. We are grateful to J.P. Gratier, Y. Méheust, Y. Géraud, M. Diraison, J.P. Vilotte, G. Batrouni, J.P. Ampuero, Y. Ben-Zion, F. Renard, and D. Marsan for fruitful discussions.

References

Bariş, S., A. Ito, S. B. Üçer, Y. Honkura, N. Kafadar, T. K. R. Pektaş, and A. M. Işikara (2002), Microearthquake activity before the Izmit earthquake in the eastern Marmara region, Turkey (1 January 1993–17 August 1999), *Bull. Seisoml. Soc. Am.*, *92*, 394–405.

Batrouni, G., A. Hansen, and J. Schmittbuhl (2002), Elastic response of rough surfaces in partial contact, *Europhys. Lett.*, *60*(5), 724–730.

Bouchon, M., H. Sekiguchi, K. Irikura, and T. Iwata (1998), Some characteristics of the stress field of the 1995 Hyogo-ken Nanbu (Kobe) earthquake, *J. Geophys. Res.*, *103*, 24,271–24,282.

Hansen, A., J. Schmittbuhl, G. Batrouni, and F. A. Oliveira (2000), Normal stress distribution of rough surfaces in contact, *Geophys. Res. Lett.*, *27*, 3639–3643.

Hansen, A., J. Schmittbuhl, and G. Batrouni (2001), Distinguishing fractional and white noise in one and two dimensions, *Phys. Rev. E*, *63*, 062102.

Lavallée, D., and R. J. Archuleta (2003), Stochastic modeling of slip spatial complexities for the 1979 Imperial Valley, California, earthquake, *Geophys. Res. Lett.*, *30*(5), 1245, doi:10.1029/2002GL015839.

Lavallée, D., and R. J. Archuleta (2005), Coupling of the random properties of the source and the ground motion for the 1999 Chi Chi earthquake, *Geophys. Res. Lett.*, *32*, L08311, doi:10.1029/2004GL022202.

Mai, P. M., and G. C. Beroza (2002), A spatial random field model to characterize complexity in earthquake slip, *J. Geophys. Res.*, *107*(B11), 2308, doi:10.1029/2001JB000588.

Méheust, Y., and J. Schmittbuhl (2001), Geometrical heterogeneities and permeability anisotropy of rough fractures, *J. Geophys. Res.*, *106*(B2), 2089–2102.

Özalaybey, S., M. Ergin, M. Aktar, C. Tapýrdamaz, F. Biçmen, and A. Yörük (2002), The 1999 Izmit earthquake sequence in Turkey: Seismological and tectonic aspects, *Bull. Seismol. Soc. Am.*, *92*, 376–386.

Power, W. L., and W. B. Durham (1997), Topography of natural and artificial fractures in granite rocks: Implications for studies of rock friction and fluid migration, *Int. J. Rock Mech. Min. Sci.*, *34*, 979–989.

Power, W. L., T. E. Tullis, S. R. Brown, G. N. Boitnott, and C. H. Scholz (1987), Roughness of natural fault surfaces, *Geophys. Res. Lett.*, *14*, 29–32.

Renard, F., J. Schmittbuhl, J. Gratier, P. Meakin, and E. Merino (2004), Three-dimensional roughness of stylolites in limestones, *J. Geophys. Res.*, *109*, B03209, doi:10.1029/2003JB002555.

Renard, F., C. Voisin, D. Marsan, and J. Schmittbuhl (2006), High resolution 3D laser scanner measurements of a strike-slip fault quantify its morphological anisotropy at all scales, *Geophys. Res. Lett.*, *33*, L04305, doi:10.1029/2005GL025038.

Rubin, A., D. Gillard, and J. Got (1999), Streaks of microearthquakes along creeping faults, *Nature*, *400*(6745), 635–641.

Schmittbuhl, J., S. Gentier, and S. Roux (1993), Field measurements of the roughness of fault surfaces, *Geophys. Res. Lett.*, *20*, 639–641.

Schmittbuhl, J., F. Schmitt, and C. Scholz (1995a), Scaling invariance of crack surfaces, *J. Geophys. Res.*, *100*, 5953–5973.

Schmittbuhl, J., J. Vilotte, and S. Roux (1995b), Reliability of self-affine measurements, *Phys. Rev. E*, *51*, 131–147.

Scholz, C. H. (1997), *The Mechanics of Earthquakes and Faulting*, Cambridge Univ. Press, New York.

Simonsen, I., A. Hansen, and O. M. Nes (1998), Using wavelet transforms for hurst exponent determination, *Phys. Rev. E*, *58*, 2779–2787.

Simonsen, I., D. Vandembroucq, and S. Roux (2000), Wave scattering from self-affine surfaces, *Phys. Rev. E*, *61*, 5914–5917.

Spudich, P. (1992), On the inference of absolute stress levels drom seismic radiation, *Tectonophysics*, *211*, 99–106.

Tinti, E., P. Spudich, and M. Cocco (2005), Earthquake fracture energy inferred from kinematic rupture models on extended faults, *J. Geophys. Res.*, *110*, B12303, doi:10.1029/2005JB003644.

M. Bouchon, Laboratoire de Géophysique Interne et Tectonique, B.P. 53, F-38041 Grenoble, France.

G. Chambon, Cemagref, Unité ETNA, Domaine Universitaire, 2 rue de la Papeterie, B.P. 76, F-38402 Saint-Martin d'Hères Cédex, France.

A. Hansen, Department of Physics, Norges Teknisk-Naturvitenskapelige Universitet, N-7491 Trondheim, Norway.

J. Schmittbuhl, Institut de Physique du Globe, UMR 7516, 5 rue René Descartes, F-67084 Strasbourg Cedex, France. (jean.schmittbuhl@eost.u-strasbg.fr)